

# Conceptual Development of Quiet Turbofan Engines for Supersonic Aircraft

Dimitri Papamoschou\*

University of California, Irvine, Irvine, California 92697-3975

and

Marco Debiasi†

The Ohio State University, Columbus, Ohio 43235

This is a joint thermodynamic and acoustic study of engines for next-generation supersonic aircraft. It explores fixed-cycle concepts with potential for quiet takeoff and efficient cruise. The flowpath is simple, without mechanical suppressors. The strategy is to take a representative state-of-the-art military turbofan engine and increase its bypass ratio to a moderate value. The engine core stays the same. Three exhaust configurations are considered: mixed flow, coaxial separate flow, and eccentric separate flow. Engine-cycle analysis predicts thermodynamic performance and nozzle exhaust conditions at takeoff and Mach 1.6 cruise. Subscale experiments duplicate the static exhaust conditions at takeoff power and measure the far-field sound. Flyover perceived noise levels are estimated for a twin-engine aircraft in the 120,000-lb class. In terms of effective perceived noise level (EPNL), the eccentric arrangement is 6.5 dB quieter than the mixed-flow arrangement and 5 dB quieter than the coaxial configuration. Spectral- and time-domain analyses indicate that the eccentric exhaust is free of strong Mach wave radiation. The acoustic benefit of the eccentric arrangement, combined with faster climb afforded by the modified engine, leads to a reduction of 14 dB in EPNL. Compared to the baseline engine, the specific fuel consumption of the modified engine is about 13% less at subsonic climb and 3% less at supersonic cruise.

## Nomenclature

$D$	= diameter
$f$	= frequency
$M$	= Mach number
$\dot{m}$	= mass flow rate
$r$	= distance from jet exit
$T$	= thrust
$t$	= time from liftoff
$U$	= velocity
$x$	= horizontal distance from brake release
$y$	= altitude
$\alpha$	= geometric angle of attack
$\gamma$	= climb angle
$\theta$	= polar angle relative to jet centerline
$\phi$	= azimuth angle relative to vertical plane
$\psi$	= polar observation angle of airplane

## Subscripts

com	= compressor
eng	= full-scale engine
exp	= subscale experiment
fan	= fan tip
LO	= liftoff
$p$	= primary (core) exhaust
$s$	= secondary (bypass) exhaust
TOM	= takeoff monitor

tot	= total
$\infty$	= flight conditions

## Introduction

COMMUNITY noise from aircraft has profound environmental and economic consequences. First-generation subsonic jetliners were very noisy because of the high exhaust velocity of their engines. Efforts to suppress noise using mixing enhancement had only moderate impact.<sup>1</sup> It was not until the introduction of the high-bypass-ratio turbofan that noise was reduced remarkably, by 20–30 dB. This was simply achieved by the same thrust being produced with a larger mass flow rate, hence lower exhaust speed. The associated gains in propulsive efficiency led to much lower fuel consumption, making the high-bypass turbofan the only choice for commercial aircraft developed in the 1980s and beyond. The increase in bypass ratio was enabled by development of high-temperature materials for the turbine blades. For given size of the gas generator, the power that can be delivered to the bypass stream is directly related to the turbine inlet temperature (TIT).

Development of economically viable supersonic transports hinges on solving the problem of community noise without penalizing aircraft performance. The same issue affects to some extent military high-performance aircraft because communities surrounding military bases are becoming increasingly sensitive to noise. So far, the bulk of the supersonic noise suppression effort has encompassed mixing enhancement and ejector approaches,<sup>2,3</sup> which typically lead to large and heavy powerplants.<sup>4</sup> One may wonder if supersonic engines will follow the same evolution as subsonic engines, leading to supersonic high-bypass turbofans. However, the issue is not as simple. High-bypass ratio generally causes worse, not better, efficiency at supersonic speeds. Figure 1 shows calculations of thrust specific fuel consumption (TSFC) and fan diameter vs bypass ratio (BPR) and fan pressure ratio (FPR) at cruise Mach number of 1.6. The calculation, based on an engine-cycle analysis mentioned later in the paper, assumes TIT = 1600 K (2400°F), a value close to today's limits of turbine materials. It is seen that the TSFC slightly dips and then rises with increasing bypass ratio. The fan diameter increases roughly with  $\sqrt{1 + \text{BPR}}$  meaning increased drag and weight of the vehicle. The quantitative information shown in Fig. 1

Presented as Paper 2002-0368 at the AIAA 40th Aerospace Sciences Meeting and Exhibit, Reno, NV, 14–17 January 2002; received 6 May 2002; revision received 21 November 2002; accepted for publication 4 December 2002. Copyright © 2003 by Dimitri Papamoschou and Marco Debiasi. Published by the American Institute of Aeronautics and Astronautics, Inc., with permission. Copies of this paper may be made for personal or internal use, on condition that the copier pay the \$10.00 per-copy fee to the Copyright Clearance Center, Inc., 222 Rosewood Drive, Danvers, MA 01923; include the code 0748-4658/03 \$10.00 in correspondence with the CCC.

\*Professor, Department of Mechanical and Aerospace Engineering, Associate Fellow AIAA.

†Postdoctoral Researcher, Mechanical Engineering, Member AIAA.

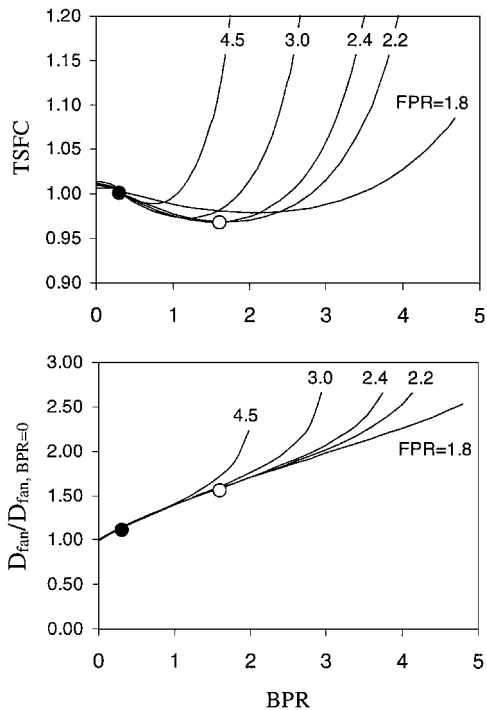


Fig. 1 TSFC and fan diameter, normalized by turbojet value, vs BPR and FPR for Mach 1.6 cruise: ●, baseline engine and ○, modified engines.

will change somewhat with the assumptions of the cycle analysis, for example, component efficiencies, but the qualitative trends will not. Figures 1 indicate that, at today's limits of TIT, bypass ratios beyond 3.0 would lead to poor performance at supersonic cruise.

Designers of supersonic engines, therefore, face two conflicting requirements: high-bypass ratio on takeoff/landing for reduced noise and low- or zero-bypass ratio for efficient supersonic cruise. One possibility is the variable-cycle turbofan engine, but it entails complexity far greater than that of today's engines. Another approach is to seek an intermediate bypass ratio that satisfies both requirements in a fixed cycle. Because the bypass ratio would be moderate, it becomes crucial how one uses the bypass stream to reduce noise. One configuration is the mixed-flow turbofan, currently used on all military engines, in which the bypass and core streams mix before exiting a common nozzle. The other option is the separate- (unmixed-) flow turbofan, which is very common on subsonic transports. The unmixed design allows shaping of the bypass exhaust so that the bypass stream substantially reduces Mach wave emission from the core stream. Previous work on the Mach wave elimination (MWE) technique showed significant gains in noise reduction by changing the shape of a dual-stream exhaust from coaxial to eccentric.<sup>5</sup>

Mach wave radiation is considered the principal source of mixing noise in supersonic jets.<sup>6–11</sup> It could also play a strong role in noise emission from high-subsonic jets due to the growth-decay nature of instability waves, which creates a spectrum of phase speeds part of which is supersonic.<sup>12,13</sup> In the MWE method, generation of Mach waves from a primary stream is suppressed by flowing a secondary parallel stream adjacent to the primary stream so that all relative eddy motions become subsonic.<sup>14</sup> Specifically, MWE seeks to minimize the convective Mach numbers of turbulent eddies throughout the jet flowfield. This includes the end of the potential core, a region of vigorous mixing and strong noise generation. In a coaxial arrangement, application of the secondary flow reduces the growth rate of the shear layer between the primary and secondary streams, thus stretching the primary potential core. The end of the primary potential core can easily extend past the reach of the secondary flow, thus reducing the effectiveness of the technique. The eccentric arrangement has been shown to prevent significant elongation of the primary potential core.<sup>15</sup> It also doubles the thickness and potential core length of the secondary flow in the downward direction,

thus making the technique very effective at suppressing Mach wave emission toward the ground. More generally, the MWE results illustrate the potential for noise reduction by shaping the mean flow of the primary and secondary streams. Our study represents the initial steps of a broader effort to reduce supersonic and subsonic jet noise by mean profile shaping of realistic engine flows.

This paper examines, at a fundamental level, the thermodynamic and acoustic performance of a fixed-cycle, moderate-bypass supersonic engine. It will be shown that significant noise reduction relative to today's military turbofan engines is achievable with an eccentric separate-flow exhaust that reduces the convective Mach number of the core stream.

## Engine Configurations

We consider a supersonic twin-engine aircraft with maximum takeoff weight of about 540 kN (120,000 lb). The assumed lift-to-drag ratio is 5 at takeoff and 10 at supersonic cruise, values roughly 20% better than those of the *Aerospatiale Concorde*.<sup>16</sup> The study starts with a representative military turbofan engine for this kind of airplane, increases its bypass ratio to moderate value, and assesses noise and performance of three configurations: the mixed-flow turbofan, the separate-flow turbofan with coaxial exhaust, and the separate-flow turbofan with eccentric exhaust. The comparison basis is the following.

1) All engines have the same supersonic cruise thrust.

2) All engines have the same core characteristics (mass flow rate to within 10%, overall pressure ratio, and turbine inlet temperature). The baseline engine is a military turbofan with BPR = 0.3, FPR = 5.0, static thrust of 126 kN (28,000 lb) and cruise thrust of 30 kN (6700 lb) at Mach 1.6 and altitude of 16,000 m. The static thrust is dictated by the federal requirement for the aircraft to climb at an angle of 1.4 deg with one engine inoperative.<sup>17</sup> The modified engines are increased mass flow rate derivatives of the baseline engine, with bypass ratio 1.6. The size, specific fuel consumption, and exhaust conditions of the engines are derived from thermodynamic analysis of a Brayton cycle with component efficiencies and specific heat ratios listed in Table 1. (See Ref. 18 for more information on the cycle analysis.) For all engines, 25–30% of the compressor air is used for turbine cooling, 1% of the compressor air is bled to systems outside the engine, and 1.5% of the turbine work drives auxiliary systems. These figures are representative of the operating conditions of modern engines. Total pressure loss due to turbine cooling is estimated at 7% times the mass fraction of cooling air.<sup>19</sup> For the mixed-flow design, the core and fan streams mix at constant pressure, constant total enthalpy, and Mach number 0.4 before expanding to ambient pressure. The overall pressure ratio (OPR) and TIT for maximum static thrust were selected at 30 and 1800 K, respectively. The requirement that all engines have the same supersonic cruise thrust sets the size of each engine. Specifically, it makes the fan diameter of each engine dependent on the OPR and TIT chosen for cruise. Because the fan diameter is a constant throughout the aircraft mission, the OPR and TIT values at takeoff define the static thrust. They were chosen such that the baseline (smallest) engine provides enough thrust for climb with one engine inoperative, that is,  $T = 126$  kN.

The engine configurations are summarized in Fig. 2. For convenience, we adopt a notation that gives the bypass ratio and type of exhaust. B16-MIX, for example, describes the bypass ratio 1.6,

Table 1 Engine cycle assumptions

Component	Efficiency	Specific heat ratio
Inlet ( $M_\infty < 1$ )	0.97	1.40
Inlet ( $M_\infty \geq 1$ )	0.85	1.40
Fan	0.85	1.40
Compressor	0.85	1.37
Combustor	1.00 <sup>a</sup>	1.35
Turbine	0.90	1.33
Nozzle	0.97	Calculation <sup>b</sup>

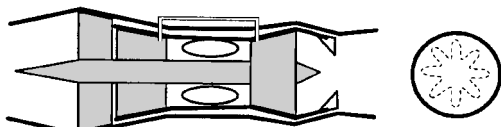
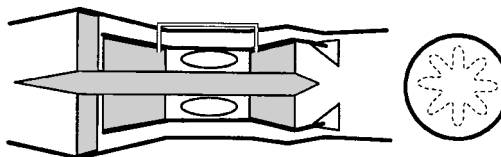
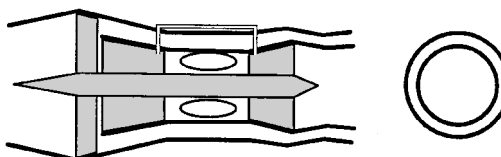
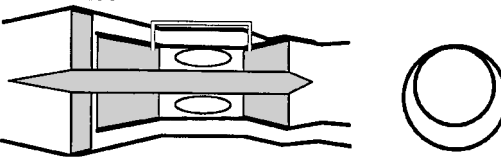
<sup>a</sup>With 5% total pressure loss. <sup>b</sup>From internal mixing calculation.

**Table 2 Engine characteristics at takeoff:**  
 $y = 0 \text{ m}$  and  $M_\infty = 0$ 

Quantity	B03-MIX	B16-SEP	B16-MIX
OPR	30	30	30
TIT, <sup>a</sup> K	1800	1800	1800
$\dot{m}_{\text{com}}$ , kg/s	125	120	115
$\dot{m}_{\text{tot}}$ , kg/s	160	303	290
$T$ , kN	126	162	159
BPR	0.30	1.60	1.60
FPR	5.0	2.6	2.6
$D_{\text{fan}}$ , <sup>b</sup> m	1.04	1.43	1.40
TSFC, 1/h	0.67	0.50	0.49 <sup>c</sup>
$M_p$	1.55	1.20	1.20
$U_p$ , m/s	770	640	530
$M_s$	—	1.20	—
$U_s$ , m/s	—	430	—

<sup>a</sup>For turbine blade cooling, 30% compressor flow.<sup>b</sup> $M = 0.5$  at fan face.<sup>c</sup>Does not account for mixer losses.**Table 3 Engine characteristics at subsonic climb:**  
 $y = 10,000 \text{ m}$  and  $M_\infty = 0.8$ 

Characteristic	B03-MIX	B16-SEP	B16-MIX
OPR	24	24	24
TIT, <sup>a</sup> K	1400	1400	1400
$\dot{m}_{\text{com}}$ , kg/s	55	63	60
$\dot{m}_{\text{tot}}$ , kg/s	85	163	156
$T$ , kN	51	55	54
BPR	0.3	1.6	1.6
FPR	4.5	2.2	2.2
$D_{\text{fan}}$ , <sup>b</sup> m	1.04	1.43	1.40
TSFC, 1/h	0.71	0.62	0.61 <sup>c</sup>
$M_p$	1.9	1.78	1.53
$U_p$ , m/s	832	819	584
$M_s$	—	1.40	—
$U_s$ , m/s	—	425	—

<sup>a</sup>For turbine blade cooling, 25% compressor flow.<sup>b</sup> $M = 0.6$  at fan face.<sup>c</sup>Does not account for mixer losses.**B03-MIX****B16-MIX****B16-SEP-COAX****B16-SEP-ECC****Fig. 2 Engine configurations.**

mixed-flow engine. The suffixes COAX and ECC indicate a coaxial or eccentric exhaust, respectively, of the separate-flow engine. For the eccentric configuration, an additional numerical suffix indicates the azimuth angle at which noise was measured. Tables 2, 3, and 4 summarize engine characteristics and thermodynamic performance at takeoff, subsonic climb, and supersonic cruise, respectively. Exhaust conditions are pressure matched for the primary stream and secondary streams. Because of their increased mass flow rate, the modified engines have 28% higher static thrust than the baseline engine. This is an important consequence of the thermodynamic cycle that needs to be dealt with as one increases the bypass ratio of supersonic engines. In other words, for the same cruise thrust, the higher-bypass engine will be inherently overpowered on takeoff. Later we take advantage of the excess thrust to enhance takeoff performance and, thus, reduce the noise footprint. At subsonic climb, the modified engines have 10% more thrust than the baseline engine, which translates into improved climb performance and faster reach of cruise altitude.

The takeoff FPR of the modified engines is 2.6, a value that presently may require a two-stage fan but in the future may be achievable with a single-stage aspirated fan.<sup>20</sup> Table 2 shows that, at

**Table 4 Engine characteristics at supersonic cruise:**  
 $y = 16,000 \text{ m}$  and  $M_\infty = 1.6$ 

Characteristic	B03-MIX	B16-SEP	B16-MIX
OPR	24	24	24
TIT, <sup>a</sup> K	1600	1600	1600
$\dot{m}_{\text{com}}$ , kg/s	55	53	51
$\dot{m}_{\text{tot}}$ , kg/s	72	137	131
$T$ , kN	30	30	30
BPR	0.3	1.6	1.6
FPR	4.5	2.2	2.2
$D_{\text{fan}}$ , <sup>b</sup> m	1.04	1.43	1.40
TSFC, 1/h	1.00	0.97	0.94 <sup>c</sup>
$M_p$	2.10	1.80	1.90
$U_p$ , m/s	890	820	700
$M_s$	—	1.95	—
$U_s$ , m/s	—	610	—

<sup>a</sup>For turbine blade cooling, 25% compressor flow.<sup>b</sup> $M = 0.7$  at fan face.<sup>c</sup>Does not account for mixer losses.

takeoff, the TSFC of the modified engines is 25% lower than that of the baseline engine. At subsonic climb (Table 3) the TSFC improvement is about 13%. At supersonic cruise (Table 4) the TSFCs of the modified engines are marginally lower than that of the baseline engine. As mentioned in the Introduction, increased bypass ratio at supersonic cruise yields only small benefits in fuel consumption. The mixed-flow turbofan has slightly better fuel consumption than the separate-flow turbofan. This calculation, however, does not include mixer losses or the added weight of the internal mixer on overall engine performance. The velocity ratio of the separate-flow exhaust at cruise,  $U_s/U_p = 0.74$ , is very close to the efficiency of energy transfer between the core and bypass flow (the product of turbine and fan efficiencies, in this case, 0.76). This indicates that B16-SEP operates at optimal cruise conditions.<sup>21</sup>

## Noise Measurement

### Facilities

Noise testing was conducted in the University of California, Irvine, Jet Aeroacoustics Facility.<sup>5</sup> Single- and dual-streamjets with flow conditions matching those given by the cycle analysis (Table 2) were produced. The jets were composed of helium-air mixtures, which duplicate very accurately the fluid mechanics and acoustics of hot jets.<sup>22</sup> Jet nozzles were fabricated from epoxy resin using rapid-prototyping techniques. Two primary (core) nozzles were designed with the method of characteristics for Mach numbers 1.5 and 1.2, matching approximately the takeoff exit Mach numbers of the baseline and modified engines, respectively. Both primary nozzles had the same exit inner diameter (14.8 mm), lip thickness (0.7 mm), and external shape. One secondary (bypass) nozzle formed a convergent duct in combination with the primary nozzle and terminated in a diameter of 21.8 mm. The pipe that fed the primary nozzle was

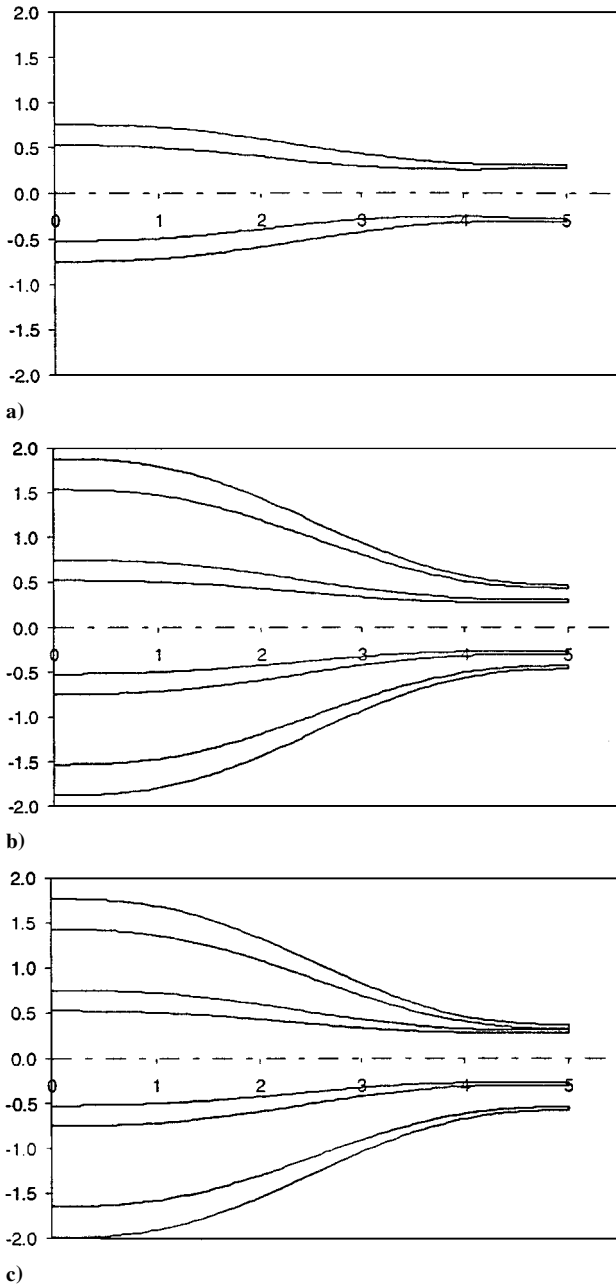


Fig. 3 Nozzle coordinates (inches) for a) B03-MIX, b) B16-SEP-COAX, and c) B16-SEP-ECC-0; nozzle for B16-MIX was the inner one alone of (b)/(c).

able to flex, enabling coaxial or eccentric secondary flow passages. The coordinates of the nozzles, are plotted in Fig. 3. For all of the nozzles, the contraction (before any supersonic expansion) was described by fifth-order polynomials and was 4:1 for the core nozzle and 15:1 for the bypass nozzle. The jet Reynolds number was on the order of  $0.5 \times 10^6$ .

Noise measurements were conducted inside an anechoic chamber using a  $\frac{1}{8}$ -in. (3.2 mm) condenser microphone (Brüel and Kjør 4138) with frequency response of 140 kHz. The microphone was mounted on a pivot arm and traced a circular arc centered at the jet exit with radius of 71 core-jet diameters. Earlier experiments have determined that this distance is well inside the acoustic far field.<sup>23</sup> The polar angle  $\theta$  ranged from 20 to 130 deg in intervals of 5 deg for  $20 \leq \theta \leq 50$  deg and 10 deg for the rest. Figure 4 shows the overall setup and the range of polar angles covered. For the eccentric jet, azimuth angles  $\phi = 0$  and 45 deg were investigated. The sound spectra were corrected for the microphone frequency response, free field response, and atmospheric absorption. All spectra were referenced to

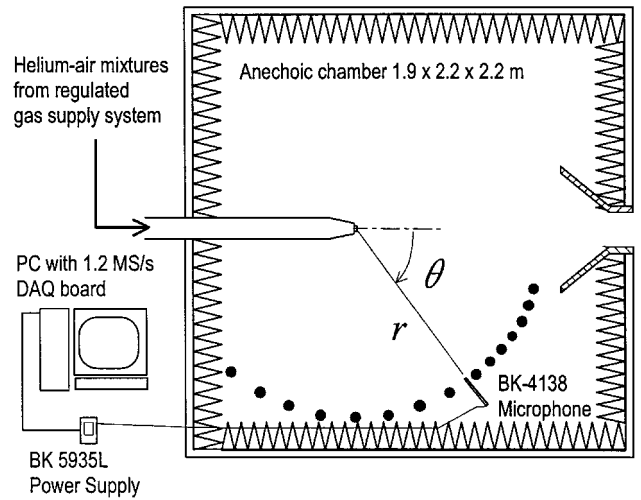


Fig. 4 Experimental setup with set of polar angles covered.

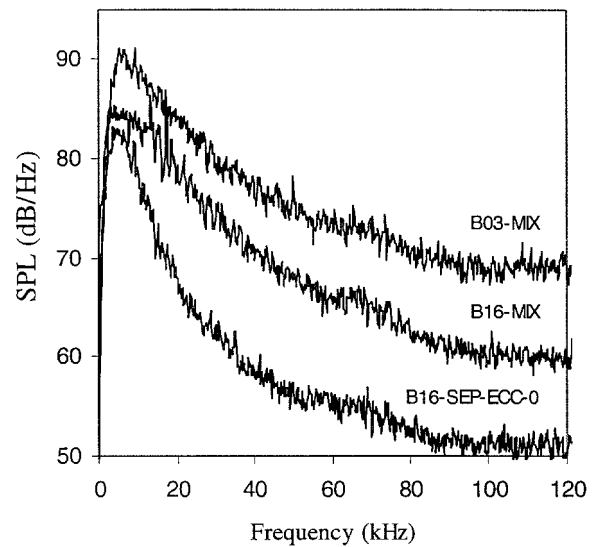


Fig. 5 Far-field spectra in the direction of peak emission, scaled to equal thrust: baseline engine ( $\theta = 40$  deg), mixed-flow derivative ( $\theta = 25$  deg), and eccentric separate-flow derivative ( $\theta = 40$  deg).

$r/D_p = 100$ . Comparison at equal thrust was done using geometric scaling.<sup>23</sup> In our facility, repetition of an experiment under varying temperature and relative-humidity conditions (typically from 20 to 50%) yields spectra that differ by at most 0.5 dB. Comparison of our single-jets spectra with those from NASA large-scale jet facilities and with the Tam et al. similarity spectra,<sup>24</sup> shows excellent agreement both in the spectral shape and in the value of overall sound pressure level (OASPL).<sup>25</sup>

### Spectra

Sound pressure level spectra are compared at equal thrust  $T = 50$  N unless otherwise noted. A frequency range of great relevance to perceived noise level is 25–75 kHz, which on a full-scale engine corresponds roughly to 500–1500 Hz, that is, the scale factor is around 50. Below this range, the human ear becomes insensitive to noise; above this range, sound gets attenuated very rapidly by atmospheric absorption. We show only spectra in the lower hemisphere of the acoustic field. As has been shown in a previous study,<sup>5</sup> noise emission of the eccentric case in the upper hemisphere matches that of the single (core) jet.

The spectra of B03-MIX, B16-MIX, and B16-SEP-ECC-0 at their respective angles of peak noise emission (aft quadrant) are compared in Fig. 5. The eccentric, separate-flow case has dramatically lower noise levels than the baseline case: about 8-dB reduction at low

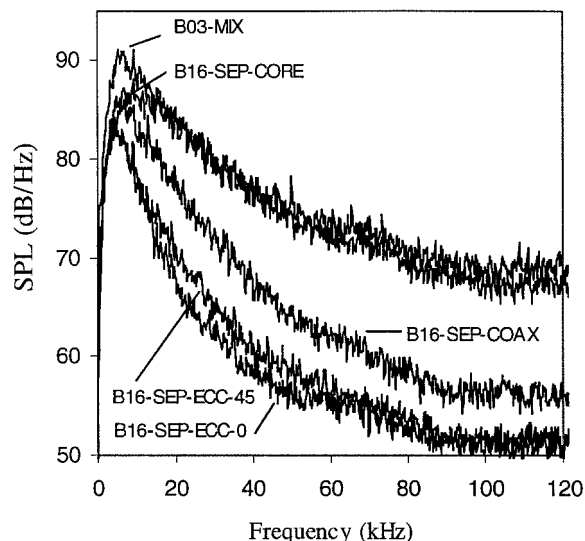


Fig. 6 Far-field spectra in the direction of peak emission ( $\theta = 40$  deg for all spectra shown), scaled to equal thrust: baseline engine, core stream alone of separate-flow derivative, coaxial separate-flow derivative, and eccentric separate-flow derivative at azimuth angles of 0 and 45 deg.

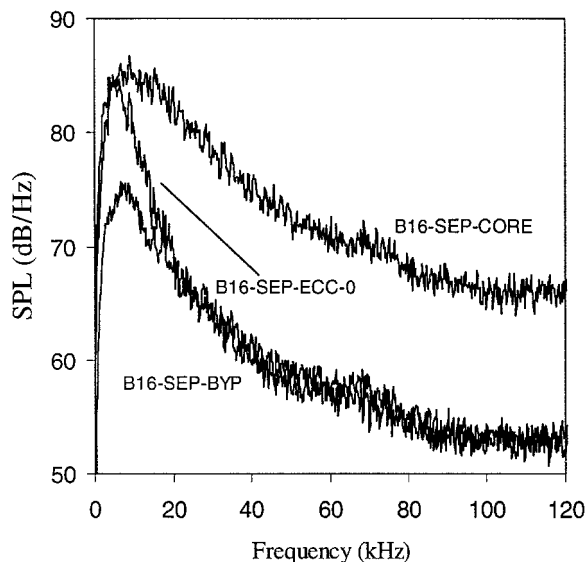


Fig. 7 Far-field spectra in the direction of peak emission ( $\theta = 40$  deg for all spectra shown), not scaled to equal thrust: eccentric separate-flow engine and its components.

frequencies and 20-dB reduction at moderate-to-high frequencies. The mixed-flow case is much louder than the separate-flow eccentric case, its spectrum exceeding that of B16-SEP-ECC-0 by 2–3 dB at  $f < 5$  kHz, 8 dB at  $f \approx 10$  kHz, and 10–12 dB for  $f > 20$  kHz. Note that an actual mixed-flow exhaust would be noisier than that shown here due to exit nonuniformities and internal noise from mixing.

The spectra of B03-MIX, B16-SEP-CORE (core stream alone), B16-SEP-COAX, B16-SEP-ECC-0, and B16-SEP-ECC-45 are compared in Fig. 6. The core stream of the modified engine is almost as loud as the exhaust of the baseline engine, except at low frequencies where it is about 3 dB quieter. (The drop in OASPL is about 2.5 dB.) The reduction in exhaust velocity from 770 to 640 m/s did not bring appreciable noise reduction. This is consistent with the sound intensity following a  $U^3$  power law, rather than  $U^8$  at lower speeds.<sup>26</sup> The separate-flow, coaxial exhaust is on average 6–8 dB louder than the eccentric exhaust. The spectra of the eccentric case at azimuth angles  $\phi = 0$  and 45 deg practically coincide, indicating that the eccentric configuration has good sideline benefit.

Figure 7 shows the spectra of B16-SEP-CORE, B16-SEP-BYP (eccentric bypass stream alone), and B16-SEP-ECC-0. The spectra

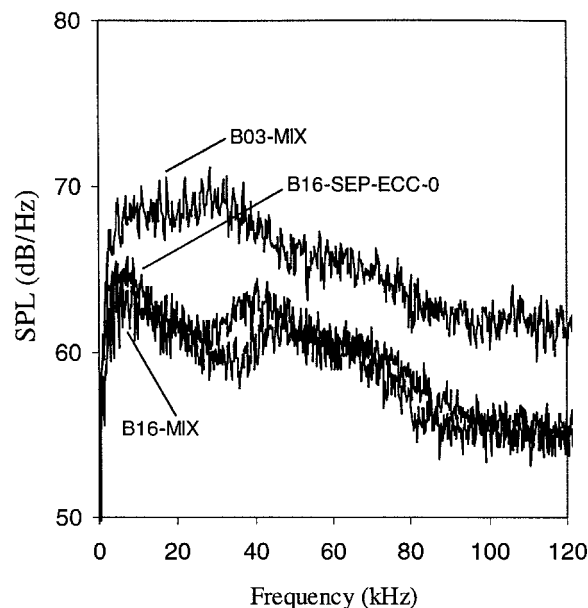


Fig. 8 Far-field spectra at  $\theta = 90$  deg: baseline engine, mixed-flow derivative, and separate-flow eccentric derivative.

are presented without equal-thrust scaling to get a clearer picture of the modification of acoustic sources. Because of its lower velocity, the fan stream is much quieter than the core stream. At frequencies above 20 kHz, the spectra of B16-SEP-ECC-0 and B16-SEP-BYP coincide, that is, the combined flow emits the same noise as the bypass stream alone. This indicates that the Mach wave emission from the core stream has been suppressed so well that the core stream is practically silent compared to the bypass stream and that the bypass stream now constitutes the noise “floor.” The effect of forward flight should lower this floor because the relative velocity of the bypass stream will reduce from 430 to about 310 m/s at climb speed. Note that the B16-SEP-BYP experiment does not represent accurately the fluid mechanics and noise emission of the bypass stream in a dual-stream jet. Instead, it attempts to establish the lower bound of noise emitted by the dual-stream jet. Experiments not covered in this paper show that the noise of B16-SEP-BYP is practically identical to that of a round or annular jet at the same velocity and Mach number.

Figure 8 shows the spectra in the lateral ( $\theta = 90$  deg) direction. The modified engines are 6–8 dB quieter than the baseline engine. The spectrum of the eccentric exhaust presents small “bumps” of 2–3 dB magnitude relative to the fully mixed exhaust. These bumps could be the result of broadband shock noise that occasionally arises in dual-stream jets,<sup>5</sup> although further investigation is needed into this issue.

#### OASPL and Skewness

Figure 9 shows the directivity of OASPL for the baseline engine and its three derivatives. The benefit of the separate-flow, eccentric exhaust is again evident. The maximum level of OASPL is reduced by 4.3 dB in B16-MIX, 5.6 dB in B16-SEP-COAX, and 10.5 dB in B16-SEP-ECC-0. In the lateral direction, for  $\theta \geq 90$  deg, the eccentric exhaust is 2–3 dB louder than the fully mixed exhaust. This increase in noise was noted in the spectrum of Fig. 8.

To gain further insight into the modification of the noise sources, we examine the acoustic signal in the time domain. Figure 10 shows the time traces of B03-MIX and B16-SEP-ECC-0 at the angle of peak emission. The signal of B03-MIX is highly skewed on the positive side and exhibits strong, irregularly spaced positive spikes. This phenomenon is associated with nonlinear formation of Mach waves in the vicinity of the source and, in a full-scale engine, is heard as “crackle.”<sup>27</sup> The signal of B16-SEP-ECC-0, on the other hand, is nearly symmetric without any spikes. The skewness of the acoustic signal allows quantification of this feature of noise, which cannot

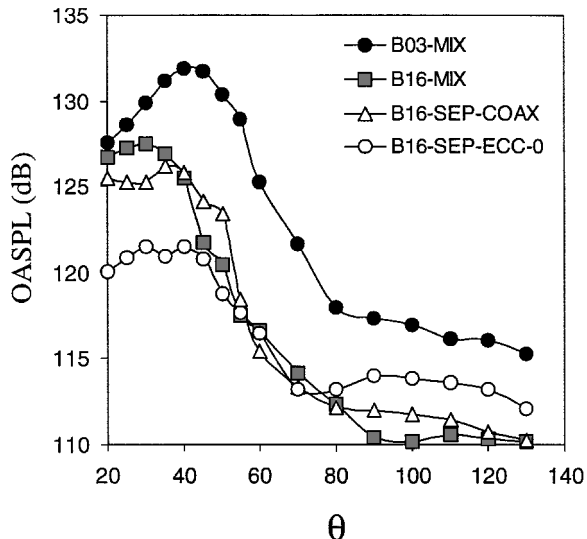


Fig. 9 Directivity of OSPL for the baseline engine and its derivatives.

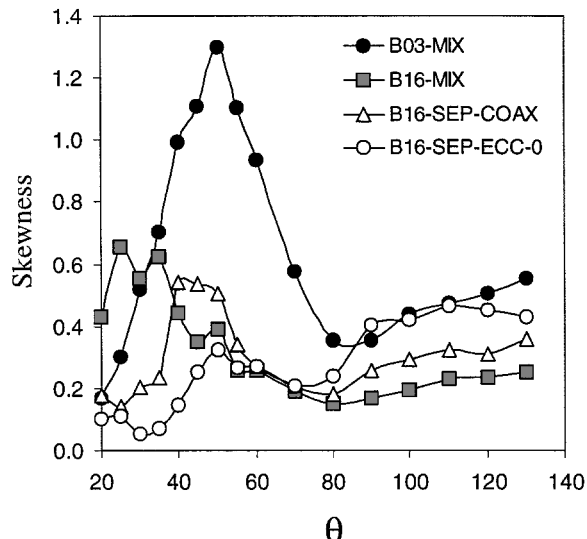


Fig. 11 Directivity of skewness for the baseline engine and its derivatives.

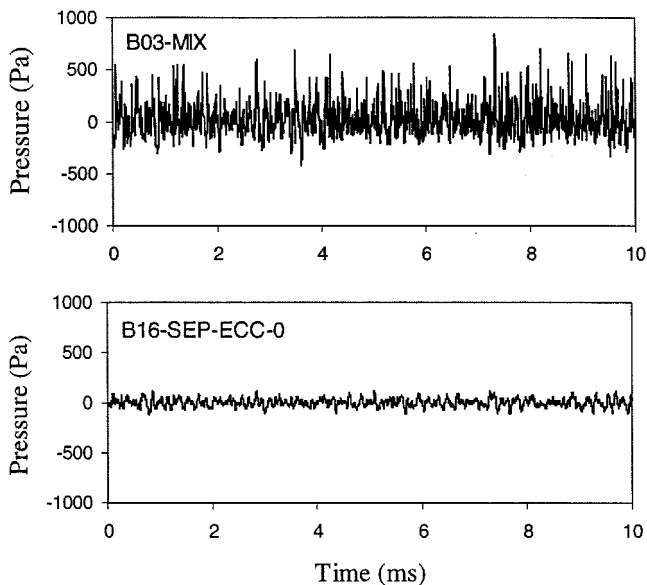


Fig. 10 Microphone time traces in the direction of peak emission for the baseline engine and the eccentric separate-flow derivative.

be captured by spectral analysis. Early work by Ffowcs-Williams et al.<sup>27</sup> has shown that high skewness is associated primarily with Mach wave emission. This was further evidenced in recent experiments by Papamoschou and Debiasi.<sup>5</sup> Ffowcs-Williams et al.<sup>27</sup> also noted that, in certain cases, high skewness was observed in the forward arc, a possible result of shock-induced noise in an imperfectly expanded jet.

Figure 11 shows the directivity of skewness for the baseline and derivative engines. The skewness of the baseline case is very high, about 1.3, at the angle of peak sound emission. The skewnesses of the mixed-flow and coaxial-exhaust cases are substantial, exceeding the threshold of 0.4. As shown by Ffowcs-Williams et al.,<sup>27</sup> this indicates that both of these cases emit significant Mach wave radiation. The skewness of B16-SEP-ECC-0 is very low in the direction of peak sound emission, consistent with elimination of Mach waves. However, it gradually rises with increasing emission angle, reaching a peak of 0.4 at  $\theta = 100$  deg. The reason for this increase is not yet understood; it may be related to broadband shock noise, as was noted in the discussion of Fig. 8. It is also instructive to compare the streams of B16-SEP-ECC separately and in combination. As shown in Fig. 12, the skewness of the core stream alone is very large, reaching 1.05 at  $\theta = 45$  deg. The skewnesses of the

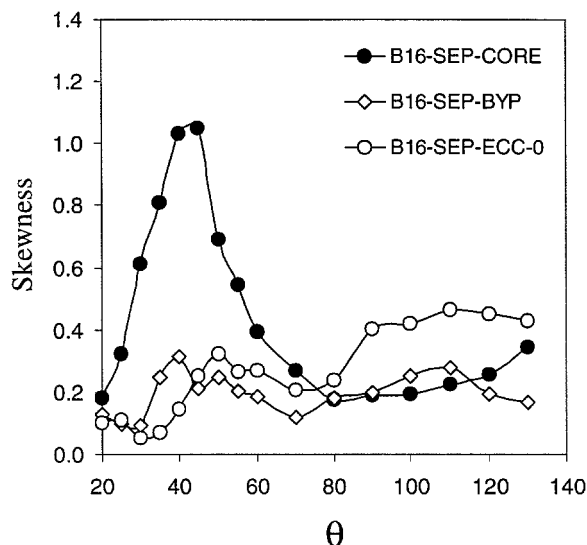


Fig. 12 Directivity of skewness for the eccentric exhaust and its components.

bypass stream alone and of the combined flow are both very low in the direction of peak sound emission, indicating that neither flow emits strong Mach waves. This is further evidence that Mach wave emission from the core stream has been substantially prevented by the eccentric bypass flow.

### Perceived Noise Level

The regulatory definition of a quiet airplane is deceptively simple. To be able to operate, an airplane must not exceed certain noise thresholds at three set locations: takeoff, sideline, and approach. Noise is quantified in terms of the effective perceived noise level (EPNL), a metric that incorporates human annoyance to sound and its duration.<sup>28</sup> EPNL thresholds are based on the configuration and weight of the airplane and stem from a mix of scientific and political considerations. As the ultimate goal of this research is development of quieter airplanes, it is essential to obtain estimates of perceived full-scale noise.

Here we attempt to process our spectra into EPNL for obtaining an assessment of perceived noise reduction. We feel that this a meaningful exercise because it includes crucial effects that are typically left out of academic studies of jet noise: distance from the source, atmospheric absorption, and human perception. The absolute levels of EPNL are not accurate because the effect of forward flight on jet

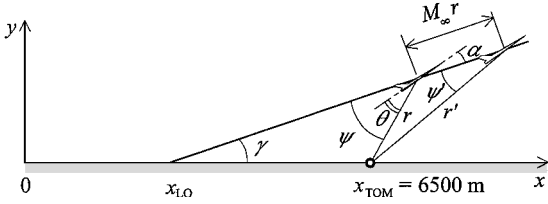


Fig. 13 Takeoff flight path with key geometric parameters.

acoustics is not present in the experiments. Other sources of noise, such as fan/compressor noise and airframe noise, are obviously not included in our assessment. We calculate noise recorded from the takeoff monitor for a full-power takeoff. Future studies will address takeoff with power cutback and noise recorded by the sideline and approach monitors.

### Flight Path

The first step in assessing perceived noise is definition of the takeoff flight path and attitude of the engines relative to the flight path. The airplanes are those defined in the “Engine Configurations” section, that is, twin engine with thrust given by the specifications of Table 2. All aircraft must have the same weight because they share the same cruise thrust. The flight path of the baseline aircraft comprises a takeoff roll  $x_{LO} = 1800$  m followed by a straight climb at angle  $\gamma = 15$  deg. The lift coefficient at climb is 0.6, which for a delta-wing aircraft corresponds to an angle of attack  $\alpha = 12$  deg (Ref. 29). The engine exhaust is assumed to be inclined at the angle of attack. The modified airplanes have 28% more takeoff thrust than the baseline case. The excess takeoff thrust can be used in two fashions: faster velocity at the same climb angle or higher climb angle at the same velocity. Here we consider the latter option. Also, takeoff roll distance is reduced by roughly the amount of thrust gain. When well-known relations for takeoff and climb performance<sup>30</sup> are used, the takeoff roll of the modified airplanes is  $x_{LO} = 1400$  m and their climb angle is  $\gamma = 23$  deg. Figure 13 shows the generic flight path with key variables.

The takeoff flight speed of all airplanes is 110 m/s ( $M_\infty = 0.32$ ). The Cartesian position  $(x, y)$  of the airplane is calculated at 0.5-s intervals from the time of liftoff. For each aircraft location, its polar coordinates  $(r, \psi)$  relative to the flight path and seen by the takeoff monitor are calculated. Here we distinguish between the apparent  $(r', \psi')$  and true  $(r, \psi)$  locations of the airplane with regard to sound emission. The apparent location is the actual location of the airplane. The true location is the one from which sound reached the observer. It is easily shown that the true position is at a distance  $M_\infty r$  behind the apparent position along the flight path. From the geometry of Fig. 13, the apparent coordinates are

$$r' = \sqrt{y^2 + (x - x_{TOM})^2}$$

$$\psi' = \pi/2 - \gamma - \arctan[(x - x_{TOM})/y]$$

and the true coordinates are obtained from

$$r = [r' / (1 - M_\infty^2)] \left[ -M_\infty \cos \psi' + \sqrt{1 - M_\infty^2 \sin^2 \psi'} \right]$$

$$\sin \psi = (r'/r) \sin \psi'$$

The polar angle of the exhaust observed by the takeoff monitor is

$$\theta = \psi - \alpha$$

When these relations are used, the true distance  $r$  and emission angle  $\theta$  are obtained as functions of time observed by the takeoff monitor.

### Data Processing

The steps for processing the laboratory narrowband spectra into perceived noise level follow.

1) The spectra are corrected to zero absorption using the relations of Bass et al.<sup>31</sup>

2) The spectra are extrapolated to frequencies higher than those resolved in the experiment (140 kHz) using a decay slope of  $-30$  dB/decade. This is done to resolve the audible spectrum for a full-scale engine. The perceived noise level (PNL) results are very insensitive on the assumed slope. Changing the slope from 0 dB/decade to  $-\infty$  dB/decade results in a 0.5 dB difference in EPNL.

3) The spectra are scaled up to engine size by dividing the laboratory frequencies by the scale factor  $\sqrt{T_{eng}/T_{exp}}$ . The full-scale engine diameter is the experimental diameter multiplied by this scale factor.

4) The spectra are Doppler shifted to account for the motion of the aircraft. The relations of McGowan and Larson<sup>32</sup> are used. In those relations, the value of the convective Mach number  $M_c$  is obtained from the empirical relations of Murakami and Papamoschou.<sup>33</sup>

5) For each observation time  $t$ , the scaled-up spectrum corresponding to  $\theta(t)$  is obtained. This step requires interpolation between spectra and, for angles outside the range covered in the experiment, moderate extrapolation. To enhance the accuracy of interpolation or extrapolation, the spectra are smoothed to remove their wiggles.

6) For each  $t$ , the corresponding scaled-up spectrum is corrected for distance and atmospheric absorption. The distance correction is

$$-20 \log_{10} \left[ \frac{(r/D_p)_{eng}}{(r/D_p)_{exp}} \right]$$

The absorption correction is applied for ambient temperature 29°C and relative humidity 70% (conditions of least absorption) using the relations of Bass et al.<sup>31</sup>

7) For each  $t$ , the corresponding scaled-up, corrected spectrum is discretized into one-third octave bands. The PNL is then computed according to part 36 of the Federal Aviation Regulations (FAR).<sup>28</sup>

8) The preceding step gives the time history of PNL,  $PNL(t)$ . From it, the maximum level of PNL (PNLM) is determined. The duration of PNL exceeding PNLM-10 dB is calculated and the corresponding “duration correction” is computed according to FAR 36. The EPNL equals PNLM plus the duration correction. The duration correction can be very substantial; hence, the importance of assessing  $PNL(t)$ . Our estimate of EPNL does not include the “tone correction,” a penalty for excessively protrusive tones in the one-third octave spectrum.

### Results

We will compare PNL time histories, and resulting EPNLs, of the baseline and modified airplanes in two ways. One is a realistic comparison that accounts for the better takeoff performance of the modified-engine aircraft. The other is an “academic” comparison in which the flight paths are identical and the engines produce the same thrust. For the latter comparison, we scale down the modified engines so that their thrust equals that of the baseline engine. Obviously the scaled-down engines do not meet the Mach 1.6 cruise requirement; hence, the academic nature of this comparison.

Figure 14 shows a comparison of PNL time histories of aircraft powered by the B03-MIX, B16-MIX, B16-SEP-COAX, and B16-SEP-ECC engines. The flight paths are identical (baseline case), and all engines produce the same thrust, 126 kN. The superiority of the separate-flow, eccentric exhaust is evident. In terms of PNLM, it is 13 dB quieter than the baseline, whereas the fully mixed and the coaxial exhausts are 5 and 6 dB quieter than the baseline, respectively. EPNL is as follows: 108.5 dB for B03-MIX, 104.5 dB for B16-MIX, 103.0 dB for B16-SEP-COAX, and 98.0 dB for B16-SEP-ECC. In other words, the eccentric separate-flow exhaust gives a 10.5 dB benefit in EPNL, whereas the mixed-flow and annular exhausts produce only 4.0 and 5.5 dB benefits, respectively.

Figure 15 shows a more realistic comparison that accounts for the higher thrust of the modified engines and resulting improved takeoff performance. The larger size of the modified engines causes a moderate increase in noise. This is more than counteracted, though, by

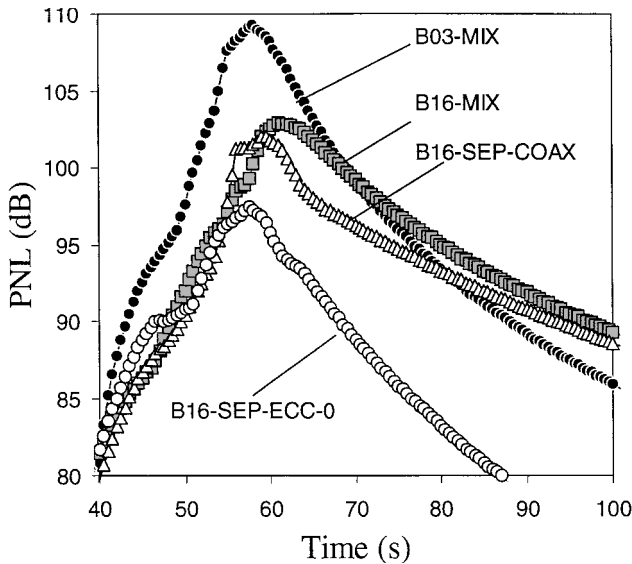


Fig. 14 Time history of flyover PNL for identical thrusts and flight paths.

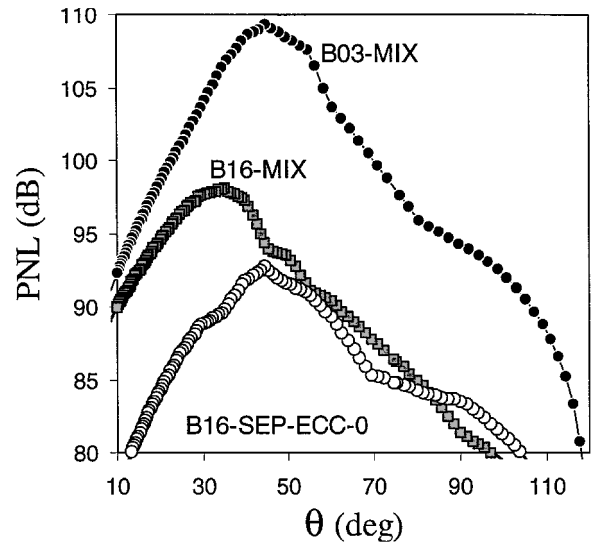


Fig. 16 Variation of PNL with emission polar angle observed by the takeoff monitor; curves correspond to time histories of Fig. 15.

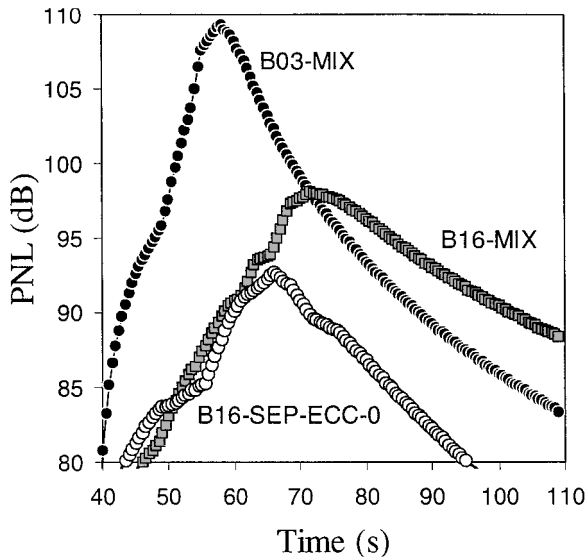


Fig. 15 Time history of flyover PNL for actual (dissimilar) thrusts and resulting different flight paths.

sound attenuation due to the higher altitude of the aircraft. The PNL histories of B03-MIX (baseline flight path), B16-MIX (enhanced flight path) and B16-SEP-ECC-0 (enhanced flight path) are plotted in Fig. 15. Comparing Figs. 14 and 15, we note that the enhanced takeoff profile produces a 3–3.5 dB attenuation in the sound from the modified aircraft, a result of their greater distance from the noise monitor. EPNL is as follows: 108.5 dB for B03-MIX, 101.5 dB for B16-MIX, and 94.5 dB for B16-SEP-ECC-0. The aircraft powered by the B16-SEP-ECC engine is, thus, 14-EPNdB quieter than that powered by the baseline B03-MIX engine.

It is also instructive to plot  $PNL(t)$  vs  $\theta(t)$  to evaluate which range of polar angles is significant to EPNL for the flow conditions considered here. This is done in Fig. 16. First, it is observed that the angles of peak PNL are very close to the angles of peak sound emission as measured in the laboratory. The aft quadrant ( $\theta < 90$  deg) is clearly very critical to EPNL because it contains all (in the case of the baseline engine) or most (in the case of the derivative engines) of the noise exceeding PNL<sub>M-10</sub>. The forward quadrant has no impact on EPNL for the baseline engine and has limited impact for the derivative engines.

## Conclusions

The possibility of a quiet, fixed-cycle supersonic turbofan engine without mechanical silencers has been explored. The assessment is preliminary and comprises thermodynamic cycle analysis, subscale acoustic measurements, and estimates of EPNL. The approach was to take a typical state-of-the-art military turbofan, increase its bypass ratio from 0.3 to 1.6, and investigate the acoustic and thermodynamic performance of several exhaust configurations. The leading configuration has a separate-flow, eccentric exhaust, which is shown to prevent strong Mach wave radiation toward the ground. An equal-thrust, equal-flight-path comparison shows that the engine with eccentric exhaust is 10.5 EPN dB quieter than the baseline engine and 6.5 EPN dB quieter than the mixed-flow engine with BPR = 1.6. When the better takeoff performance of an airplane powered by the modified engines is accounted for, the eccentric exhaust gives a 14-EPNdB benefit relative to the baseline engine. Specific fuel consumption at Mach 1.6 supersonic cruise is about 3% better than baseline. The modified engines have a fan diameter 37% larger than the baseline engine. This will require careful integration of the engine with the airframe to avoid substantial increases in wave drag due to the increased nacelle size. In the case of the eccentric exhaust, internal losses due to the nonconcentric arrangement must be carefully assessed.

The study does not include the effect of forward flight on acoustics because the University of California, Irvine, laboratory is not equipped with a tertiary stream. Forward flight is expected to enhance the noise benefit of the eccentric exhaust. Examination of the spectra shows that, except at very low frequencies, noise from the eccentric exhaust is dominated by that of the secondary (bypass) stream (Fig. 7). Forward speed at takeoff will reduce the relative velocity of the bypass stream from 430 to 310 m/s, a 28% drop. Using the simple argument that, at this low velocity, sound intensity is proportional to relative velocity raised to the eighth power,<sup>26</sup> we expect a noise reduction of 11.5 dB. In contrast, the relative velocity of the mixed-flow exhaust will reduce by only 23% (from 530 to 410 m/s), leading to a noise reduction of 9 dB. These preliminary arguments suggest that the noise benefit of the separate-flow, eccentric exhaust relative to the mixed-flow exhaust will widen with increasing flight Mach number. Moreover, classical relations for shear layer growth rate<sup>15</sup> indicate that forward speed will stretch the potential core of the bypass stream further than that of the core stream, yielding better coverage of the core stream by the bypass stream. It is hoped that large-scale experiments in government or industry facilities will address these issues.



## Acknowledgments

The support by NASA John H. Glenn Research Center is gratefully acknowledged (Grant NAG-3-2345 monitored by Khairul B. Zaman). We also thank Erin Abbey for her work on rapid prototyping of the jet nozzles and for running the experiments presented here.

## References

- <sup>1</sup>Smith, M. J. T., *Aircraft Noise*, 1st ed., Cambridge Univ. Press, Cambridge, England, U.K., 1989, pp. 120–134.
- <sup>2</sup>Nagamatsu, H. T., Sheer, R. E., and Gill, M. S., “Characteristics of Multitude Multishroud Supersonic Jet Noise Suppressor,” *AIAA Journal*, Vol. 10, No. 3, 1972, pp. 307–313.
- <sup>3</sup>Tillman, T. G., Paterson, R. W., and Presz, W. M., “Supersonic Nozzle Mixer Ejector,” *Journal of Propulsion and Power*, Vol. 8, No. 2, 1992, pp. 513–519.
- <sup>4</sup>Plencner, R. M., “Engine Technology Challenges for the High-Speed Civil Transport Plane,” AIAA Paper 98-2505, June 1998.
- <sup>5</sup>Papamoschou, D., and Debiasi, M., “Directional Suppression of Noise from a High-Speed Jet,” *AIAA Journal*, Vol. 39, No. 3, 2001, pp. 380–387.
- <sup>6</sup>Troutt, T. R., and McLaughlin, D. K., “Experiments on the Flow and Acoustic Properties of a Moderate Reynolds Number Supersonic Jet,” *Journal of Fluid Mechanics*, Vol. 116, March 1982, pp. 123–156.
- <sup>7</sup>Tam, C. K. W., Chen, P., and Seiner, J. M., “Relationship Between Instability Waves and Noise of High-Speed Jets,” *AIAA Journal*, Vol. 30, No. 7, 1992, pp. 1747–1752.
- <sup>8</sup>Tam, C. K. W., and Chen, P., “Turbulent Mixing Noise from Supersonic Jets,” *AIAA Journal*, Vol. 32, No. 9, 1994, pp. 1774–1780.
- <sup>9</sup>Tam, C. K. W., “Supersonic Jet Noise,” *Annual Review of Fluid Mechanics*, Vol. 27, 1995, pp. 17–43.
- <sup>10</sup>Seiner, J. M., Bhat, T. R. S., and Ponton, M. K., “Mach Wave Emission from a High-Temperature Supersonic Jet,” *AIAA Journal*, Vol. 32, No. 12, 1994, pp. 2345–2350.
- <sup>11</sup>Mitchell, B. E., Lele, S. K., and Moin, P., “Direct Computation of Mach Wave Radiation in an Axisymmetric Supersonic Jet,” *AIAA Journal*, Vol. 35, No. 10, 1994, pp. 1574–1580.
- <sup>12</sup>Crighton, D. G., and Huerre, P., “Shear-Layer Pressure Fluctuations and Superdirective Acoustic Sources,” *Journal of Fluid Mechanics*, Vol. 220, 1990, pp. 355–368.
- <sup>13</sup>Avital, E. J., Sandham, N. D., and Luo, K. H., “Mach Wave Radiation in Mixing Layers. Part I: Analysis of the Sound Field,” *Theoretical and Computational Fluid Dynamics*, Vol. 12, No. 2, 1998, pp. 73–90.
- <sup>14</sup>Papamoschou, D., “Mach Wave Elimination from Supersonic Jets,” *AIAA Journal*, Vol. 35, No. 10, 1997, pp. 1604–1611.
- <sup>15</sup>Murakami, E., and Papamoschou, D., “Mean Flow Development in Dual-Stream Compressible Jets,” *AIAA Journal*, Vol. 40, No. 6, 2002, pp. 1131–1138.
- <sup>16</sup>Mair, W. A., and Birdsall, D. L., *Aircraft Performance*, 1st ed., Aerospace Series 5, Cambridge Univ. Press, Cambridge, England, U.K., 1992, pp. 260, 261.
- <sup>17</sup>“Airworthiness Standards: Transport Category Aircraft: Climb: One-Engine-Inoperative,” Federal Aviation Regulations Pt. 25.121, Federal Aviation Administration, Jan. 2002.
- <sup>18</sup>Debiasi, M., and Papamoschou, D., “Cycle Analysis for Quieter Supersonic Turbofan Engines,” AIAA Paper 2001-3749, July 2001.
- <sup>19</sup>Horlock, J. H., Watson, D. T., and Jones, T. V., “Limitations on Gas Turbine Performance Imposed by Large Turbine Cooling Flows,” *Journal of Engineering for Gas Turbines and Power*, Vol. 123, No. 3, 2001, pp. 487–494.
- <sup>20</sup>Lord, W. K., MacMartin, D. G., and Tillman, T. G., “Flow Control Opportunities in Gas Turbine Engines,” AIAA Paper 2000-2234, June 2000.
- <sup>21</sup>Guha, A., “Optimum Fan Pressure Ratio for Bypass Engines with Separate or Mixed Flow Exhaust Streams,” *Journal of Propulsion and Power*, Vol. 17, No. 5, 2001, pp. 1117–1122.
- <sup>22</sup>Kinzie, K. W., and McLaughlin, D. K., “Measurements of Supersonic Helium/Air Mixture Jets,” *AIAA Journal*, Vol. 37, No. 11, 1999, pp. 1363–1369.
- <sup>23</sup>Papamoschou, D., and Debiasi, M., “Noise Measurements in Supersonic Jets Treated with the Mach Wave Elimination Method,” *AIAA Journal*, Vol. 37, No. 2, 1999, pp. 154–160.
- <sup>24</sup>Tam, C. K. W., Golebiowski, M., and Seiner, J., “On the Two Components of Turbulent Mixing Noise from Supersonic Jets,” AIAA Paper 96-1716, 1996.
- <sup>25</sup>Tam, C. K. W., “Review of Noise Data and Recent Advances in Jet Noise Theory,” *Proceedings of the Jet Noise Workshop*, NASA CP-2001-211152, Cleveland, Nov. 2002, pp. 143–183.
- <sup>26</sup>Dowling, A. P., and Ffowcs Williams, J. E., *Sound and Sources of Sound*, Halsted, New York, 1983, pp. 159–163.
- <sup>27</sup>Ffowcs Williams, J. E., Simson, J., and Virchis, V. J., “Crackle: an Annoying Component of Jet Noise,” *Journal of Fluid Mechanics*, Vol. 71, Pt. 2, 1975, pp. 251–271.
- <sup>28</sup>“Noise Standards: Aircraft Type and Airworthiness Certification,” Federal Aviation Regulations Pt. 36, Federal Aviation Administration, Jan. 2001.
- <sup>29</sup>Bertin, J. J., and Smith, M. L., *Aerodynamics for Engineers*, 3rd ed., Prentice-Hall, Upper Saddle River, NJ, 1998, pp. 319–321.
- <sup>30</sup>Shevell, R. S., *Fundamentals of Flight*, Prentice-Hall, Upper Saddle River, NJ, 1989, pp. 265, 293.
- <sup>31</sup>Bass, H. E., Sutherland, L. C., Zuckerwar, A. J., Blackstock, D. T., and Hester, D. M., “Atmospheric Absorption of Sound: Further Developments,” *Journal of the Acoustical Society of America*, Vol. 97, No. 1, 1995, pp. 680–683.
- <sup>32</sup>McGowan, R. S., and Larson, R. S., “Relationship Between Static, Flight and Simulated Flight Jet Noise Measurements,” *AIAA Journal*, Vol. 22, No. 4, 1984, pp. 460–464.
- <sup>33</sup>Murakami, E., and Papamoschou, D., “Eddy Convection in Supersonic Coaxial Jets,” *AIAA Journal*, Vol. 38, No. 4, 2000, pp. 628–635.